European Review for Medical and Pharmacological Sciences 2020; 24: 4855-4862

Involvement of microRNA-124 in biological behaviors of laryngeal carcinoma *via* PLOD2 signaling pathway

J. HUANG, X.-H. ZHOU, S. HUANG, S. LI, T.-T. WU

Department of Otolaryngology Head and Neck Surgery, Zhongnan Hospital of Wuhan University, Wuhan, China

Abstract. – OBJECTIVE: The purpose of this study was to investigate the role of microRNA-124 (miR-124) in laryngeal carcinoma (LC) and to explore the underlying mechanisms.

PATIENTS AND METHODS: LC tissues were collected from 98 patients diagnosed with LC in our hospital. Quantitative Real Time-Polymerase Chain Reaction (qRT-PCR) analysis was used to detect the expression levels of miR-124 and procollagen-lysine, 2-oxoglutarate 5-dioxygenase 2 (PLOD2) in LC tissues and cell lines. Bioinformatics (TargetScan and miRDB) and double Luciferase assay were performed to predict and confirm the relationship between PLOD2 and miR-124 in LC, respectively. MTT (3-(4,5-dimethylthiazol-2-yl)-2,5-diphenyl tetrazolium bromide) assay and the colony formation assay were designed to measure the proliferation ability of the cells. Additionally, transwell and wound healing assays were used to explore cell migration and invasion.

RESULTS: MiR-124 was found significantly downregulated both in LC tissues and cells. PLOD2 was predicted and confirmed as the target gene of miR-124 in LC. By regulating the protein expression of PLOD2, miR-124 could significantly suppress the proliferation, migration, and invasion of cells. However, the transfection of PLOD2 could partially offset the effects of miR-124 on LC cells.

CONCLUSIONS: MiR-124 was involved in regulating the malignant behaviors of LC cells. Furthermore, the miR-124/PLOD2 axis might become a potential target for the treatment of LC.

Key Words:
Laryngeal carcinoma (LC), MicroRNA-124 (miR-124), Procollagen-lysine, 2-oxoglutarate 5-dioxygenase2 (PLOD2).

Introduction

Currently, the morbidity rate of head-neck malignant tumors ranks sixth among all malignant tumors, seriously endangering people's health[1]. Laryngeal carcinoma (LC) is one of the most common head-neck malignant tumors. The morbidity rate of LC ranks second in malignant tumors of the upper respiratory tract[2]. With the rapid development of the modern medical technology, great progress has been made in clinical diagnosis and treatment of LC[3-5]. However, due to complex biological behaviors and diverse clinical manifestations, its early diagnosis rate still remains low. Meanwhile, there are many postoperative complications with high recurrence rate[6,7]. In view of this, searching for effective methods for early diagnosis of LC and effective therapeutic measures have been the key and difficulty in LC research.

MicroRNAs (miRNAs) are a class of non-coding RNAs with 19-25 nucleotides in length[8,9]. It can reduce the expression level of mRNAs or inhibit the translation of target genes by pairing with the 3' non-transcribed region (3'UTR) of the target genes[10,11]. Functionally, miRNAs are involved in cell proliferation[12,13], differentiation[14], apoptosis[15,16], and migration[17]. MiRNAs can be considered as oncogenes or tumor suppressor genes since they are involved in tumor formation, cell invasion, and angiogenesis[18-20]. MiR-124 has been confirmed[21-23] to play an important role in hepatocellular carcinoma, thyroid carcinoma[24], renal cell carcinoma[25], and non-small cell lung cancer[26]. However, no studies have investigated the relationship between miR-124 and LC.

In this paper, we first detected the expression level of miR-124 in LC tissues and cells. Furthermore, we investigated the effect of miR-124 on biological behaviors of LC cells and the underlying mechanism.

Patients and Methods

Tissue Samples

This study was approved by the Ethics Committee of Zhongnan Hospital of Wuhan University. 98 paired LC tissues, and normal laryngeal tis-

Corresponding Author: Tingting Wu, MD; e-mail: tingtingwu0310@outlook.com

sues were collected by LC patients who received surgery from May 2016 to December 2018 in our hospital. The collected tissues were immediately stored in liquid nitrogen for use. All patients were pathologically diagnosed with LC using paraffin sections. Informed consent was obtained from patients before the operation.

Cell Culture and Transfection

LC cell line (Hep-2) and human immortalized epidermal cells (HaCaT) were obtained from American Type Culture Collection (ATCC; Manassas, VA, USA). All cells were cultured in Roswell Park Memorial Institute-1640 (RPMI-1640) medium (HyClone, South Logan, UT, USA) containing 10% fetal bovine serum (FBS; Gibco, Rockville, MD, USA) in an incubator with 5% CO_2 at 37°C. The original medium was replaced with fresh medium at 24 h. When the cells covered the bottom of the culture-plates, they were digested with 0.25% trypsin, followed by cell passage. Hep-2 cells in the logarithmic growth phase were transfected with miRNA-NC, miRNA-mimics, miRNA-inhibitor, and PLOD2 according to the instructions of Lipofectamine 2000 (Lipo2000; Invitrogen, Carlsbad, CA, USA), respectively. Before refreshed with normal growth medium 6 h later, the cells were incubated in the serum-free medium. Finally, the transfected cells were collected for subsequent functional assays after 48 h.

Target Gene Prediction

Bioinformatics (TargetScan and miRDB) were used to predict the target genes of miR-124. To confirm the prediction, the plasmids containing PLOD2-wild-type (PLOD2-WT) + Negative control (miR-NC), PLOD2-WT + miR-124 mimic, PLOD2-mutant-type (PLOD2-MUT) + miR-NC, and PLOD2-MUT+ miR-124 mimic were co-transfected into Hep-2 cells (1.5×10^5 cells/well), respectively. After 48 h of culture, the cells in each group were assayed according to the manufacturer's instructions of the Dual-Luciferase Assay System (Promega, Madison, WI, USA).

RNA Extraction and Quantitative Real Time-Polymerase Chain Reaction (q-PCR) Analysis

The cells were lysed in an Eppendorf (EP) tube containing 500 μL of lysis buffer. The total RNA in the cells was extracted using TRIzol reagent (Invitrogen, Carlsbad, CA, USA). Subsequently, 1 μg of total RNA was synthesized into complementary deoxyribose nucleic acid (cDNA) according to the instructions. U6 and glyceraldehyde 3-phosphate dehydrogenase (GAPDH) were used as internal references for miRNAs and mRNAs, respectively. The specific reaction conditions were as follows: 95°C for 1 min, 95°C for 15 s, and 60°C for 1 min, for a total of 40 cycles. According to the instructions of the qPCR reagent (TaKaRa, Otsu, Shiga, Japan), the expression levels of miR-124 and PLOD2 were calculated based on $RQ=2^{-\Delta\Delta CT}$. The primer sequences used in this study were as follows: PLOD2, F: 5'-CGAAGCAGGCCTCCTCTACATC-3', R: 5'-CGAGCCGATGTGTAAGTAGGA-3'; microRNA-124, F: 5'-GAGAGGCCTGTACACGACATG-3', R: 5'-AGGTTAGTGAGTGAGTAG-3'; U6: F: 5'-GCTTCGGCAGCACATATACTAAAAT-3', R: 5'-CGCTTCAGAATTTGCGTGTCAT-3'; GAPDH: F: 5'-CGCTCTCTGCTCCTCCTGTTC-3', R: 5'-ATCCGTTGACTCCGACCTTCAC-3'.

Western Blot Analysis

Prepared sodium dodecyl sulphate-polyacrylamide gel electrophoresis (SDS-PAGE) gel was first put into the vertical electrophoresis tank. An appropriate volume of protein sample (about 40 μg) was added to the wells according to the protein concentration to ensure the same amount of protein in each well. Then, the protein samples were separated by electrophoresis and transferred onto polyvinylidene difluoride (PVDF) membranes (Roche, Basel, Switzerland). Then, the PVDF membranes were blocked with Tris-Buffered Saline and Tween 20 (TBST-20) solution containing 8% skim milk for 1 h at room temperature. Thereafter, the membranes were incubated with primary antibodies of PLOD and GAPDH in TBST solution containing 5% skim milk at 4°C overnight. On the next day, the membranes were incubated with the corresponding secondary antibody for 1 h at room temperature. Then, the membranes were rinsed with TBST for 10 min three times. Next, the membranes were added with mixed enhanced chemiluminescence (ECL) reagents A and B in a 1:1 ratio. The immunoreactive bands were finally exposed.

MTT (3-(4,5-Dimethylthiazol-2-yl)-2,5-Diphenyl Tetrazolium Bromide) Assay

After transfection, Hep-2 cells in the logarithmic growth phase were digested with trypsin and prepared into single-cell suspension. Then, the cells were inoculated into 96-well plates at a density of 1×10^3 cells/well. After culture for 7 d, 20 μL of MTT solution (Sigma-Aldrich, Saint Louis, MO, USA) was added into each well and

mixed evenly, followed by incubation at 37°C for 4-6 h. The supernatant in each well was then mixed evenly with 150 μL of dimethyl sulfoxide (DMSO; Sigma-Aldrich, Saint Louis, MO, USA). Absorbance at 490 nm was measured at 24, 48, 72, and 96 h, respectively. Finally, the cell proliferation curve was plotted.

Colony Formation Assay

Colony formation assay was used to study the long-term influence of miR-124 on Hep-2 cell proliferation. Briefly, Hep-2 cells were seeded into 6-well plates at a density of 1×10^3 cells/well. Then, the cells were cultured in a constant temperature incubator. 10 days later, the cells were washed with phosphate-buffered saline (PBS) and fixed with 4% paraformaldehyde solution for 15 minutes, followed by staining with 1% crystal violet solution. Formed colonies (> 50 cells) were observed under a light microscope, and the number of colonies was counted and analyzed.

Transwell Assay

The cells were first inoculated into 6-well plates and transfected. After 24 h, the cells were digested and blown into cell suspension using the serum-free and double antibody-free medium. The cell concentration was then adjusted. 100 μL of cell suspension and 650 μL of complete medium were added into the upper and lower chambers, respectively, followed by incubation at 37°C for 24 h. Subsequently, the cells were fixed with formaldehyde solution, stained with hematoxylin, and washed with PBS. After wiped clean with a cotton swab, the cells were sealed with neutral resins. After drying, the cells were observed and photographed under a microscope (40×). Finally, the number of migrating or invading cells was counted.

Would Healing Assay

Hep-2 cells were seeded into 6-well plates and transfected until about 70% of cell conference. The medium was changed with 10% FBS Dulbecco's Modified Eagle's Medium (DMEM; Gibco, Rockville, MD, USA) 6-8 h later. After 6 h of culture, the dead cells were gently washed away with PBS. Meanwhile, the wells in the plate were streaked with a 100 μl tip, and the force was evenly applied. After streaking, the cells were gently rinsed with PBS and replaced with 2 mL serum-free DMEM medium. The scratches were photographed immediately after streaking the line. The cells were re-exchanged every 24 h, and the scratches were photographed at 48 h. According to the variation of the width and the width of scratches between different groups, the migration and invasiveness of each group were determined.

Statistical Analysis

GraphPad Prism 7.0 software (La Jolla, CA, USA) was used for all statistical analysis. *t*-test was used for analyzing measurement data. Student's *t*-test was applied to compare the difference between the two groups. One-way ANOVA was used to compare the differences among different groups, followed by the post-hoc test (Least Significant Difference). $p<0.05$ was considered statistically significant.

Results

Expression Level of MiR-124 in LC Tissues and Hep-2 Cells

Based on previous studies, we realized that miRNA-124 might have a great influence on the development of tumor cells. Therefore, we first detected the expression level of miRNA-124 in LC tissues and adjacent normal tissues. QRT-PCR results showed that the expression level of miRNA-124 was significantly downregulated in LC tissues when compared with adjacent normal tissues (Figure 1A). Similarly, miR-124 expression in Hep-2 cells was significantly lower than that of HaCaT cells (Figure 1B). These results strongly suggested that miR-124 might be involved in the progression of LC.

PLOD2 Was a Target Gene of MiR-124

Bioinformatics (TargetScan and miRDB) predicted that miR-124 could combine with the segments of 189-195 in PLOD2 3'UTR (as shown in Figure 2A), thereby playing a regulatory role in LC cells *via* PLOD2. Therefore, wild-type (WT) and mutant-type (MUT) PLOD2 were designed, and co-transfected into cells with miR-124 mimics or miR-NC, respectively. Luciferase activity was detected *via* Dual-Luciferase Reporter Gene Assay. The results showed that the fluorescence intensity was significantly lower in the cells transfected with PLOD2-WT and miR-124 mimics. However, no evident differences were observed in PLOD2-MUT treated cells (Figure 2B). QRT-PCR results indicated that no significant differences were observed in PLOD2 mRNA expression level among the three groups (Figure 2C). However, the protein expression of PLOD2 in

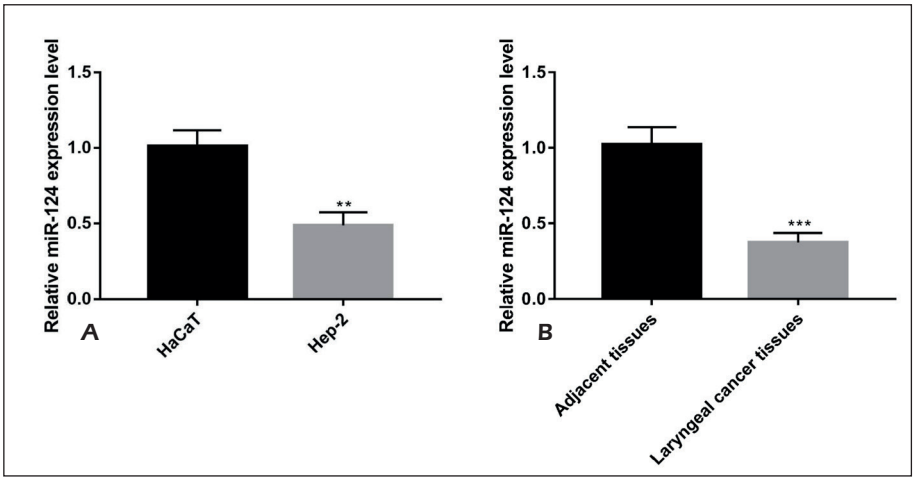

Figure 1. MiR-124 expression level in LC tissues and cells. **A**, MiR-124 expression level was downregulated in both LC tissues **A**, and cells **B**, compared with adjacent normal tissues and HaCaT cells, respectively. (**p<0.01, ***p<0.001 *vs.* control group).

Hep-2 cells transfected with miR-124 mimic was significantly downregulated when compared with the control cells. Meanwhile, the cells transfected with miR-124 inhibitor showed a reversed manner compared with the control cells (Figures 2D, 2E). All these findings suggested that miR-124 regulated PLOD2 expression at the post-transcriptional level.

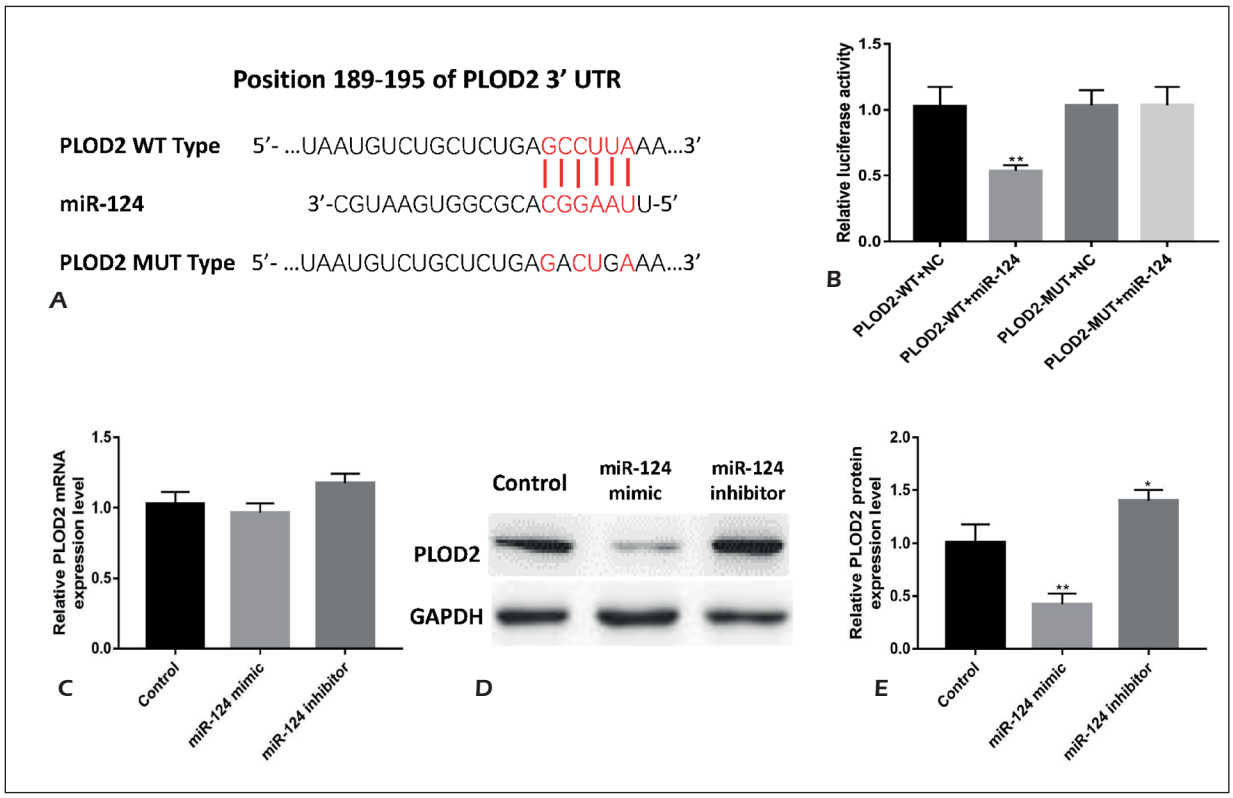

Figure 2. PLOD2 was a target gene of miR-124. **A**, MiR-124 combined segments of 189-195 in PLOD2 3'UTR. **B**, Relative Luciferase activity. **C**, The mRNA expression level of PLOD2 showed no significant differences in the cells transfected with miR-124 mimics or inhibitor compared with the control group. **D**, Protein expression level of PLOD2 in cells after transfection of miR-124 mimics or inhibitor were significantly downregulated or upregulated when compared with normal cells, respectively. **E**, Qualification of protein expression level of PLOD2. (**p<0.01, ***p<0.001 *vs.* control group).

PLOD2 Restored the Inhibitory Effect of MiR-124 on LC Cells

To further investigate the effects of miR-124 and PLOD2 on LC cells, control group, miR-124 mimic group (Hep-2 cells transfected with miR-124 mimic), and miR-124 mimic+PLOD2 group (Hep-2 cells co-transfected with miR-124 mimic and LV-PLOD2) were established. MTT assay and colony formation assay (shown in Figure 3) demonstrated that the proliferation ability of LC cells transfected with miR-124 mimics was significantly suppressed when compared with the control group. After the overexpression of miR-124 and PLOGD2, the impaired proliferation ability could be significantly rescued. In spite of this, subsequent transwell and wound healing assays indicated that the invasion and migration of LC cells were significantly inhibited in the miR-124 mimic group. Furthermore, these inhibitory effects could be alleviated by recovering PLOD2 expression in LC cells (Figure 4).

All the above findings indicated that miR-124 could inhibit the proliferation, invasion, and migration of LC cells. Meanwhile, the upregulation of PLOD2 expression in cells could counteract the role of miR-124 in cells.

Discussion

LC is a common head-neck malignant tumor, with multi-gene abnormality and strong invasion. It accounts for about 2.4% in new tumor cases every year[27]. With the emergence and develop-

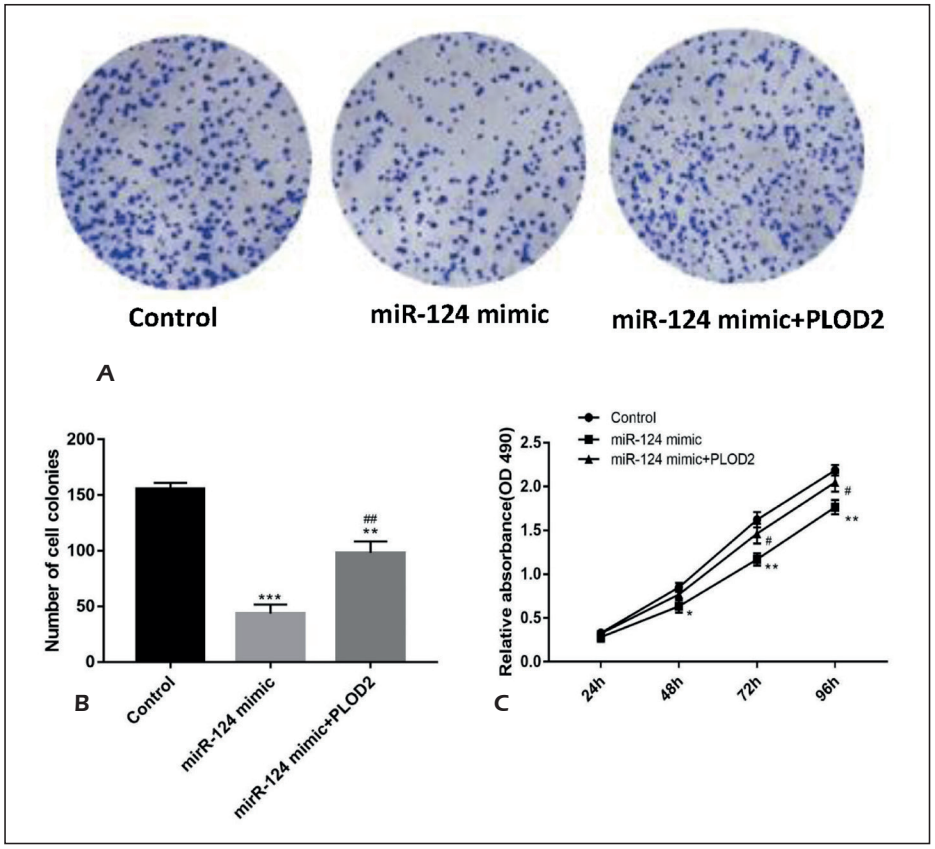

Figure 3. Effects of miR-124 and PLOD2 on the proliferation ability of LC cells detected by colony formation assay and MTT assay. **A**, Three different groups of colony formation assay were observed under a microscope (magnification x 40). **B**, The number of colonies in miR-124 mimic group was significantly reduced when compared with the control group. However, the overexpression of PLOD2 could partially restore this effect. **D**, MTT assay showed that miR-124 could inhibit the proliferation ability of LC cells, while PLOD2 could counteract this effect. (*p<0.05, **p<0.01, ***p<0.001 *vs.* control group, $^{\#}p$<0.05, $^{\#\#}p$<0.01 *vs.* miR-124 mimic group).

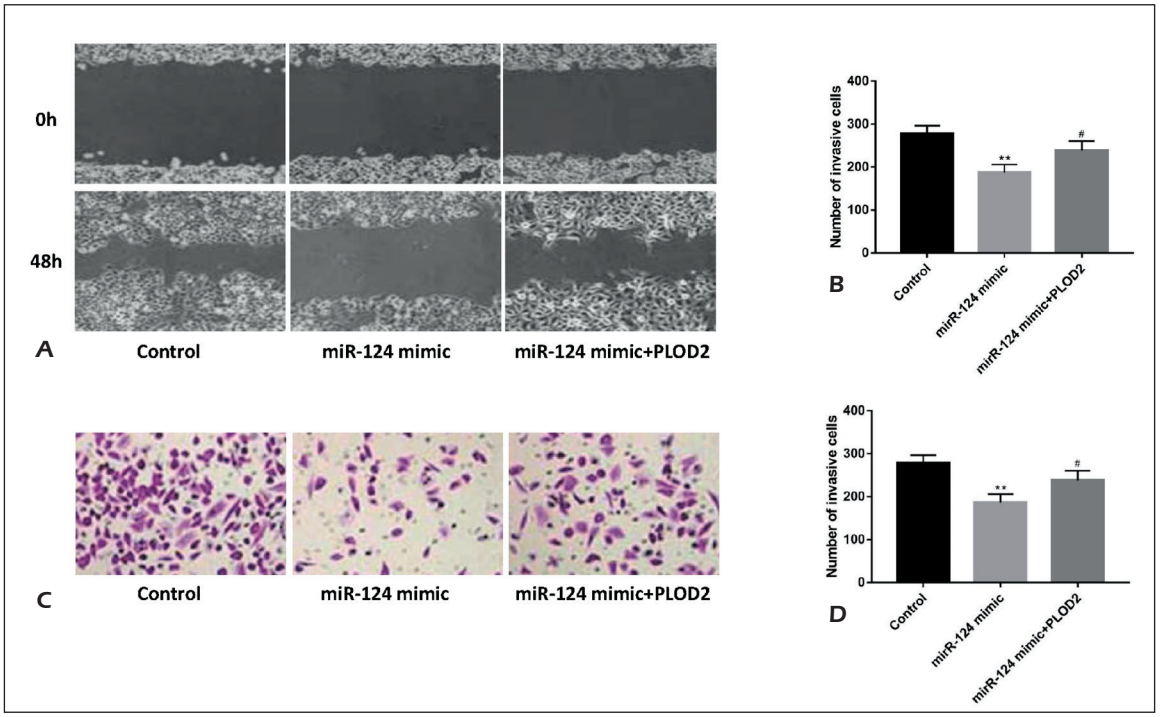

Figure 4. Effects of miR-124 and PLOD2 on the migration and invasion ability of LC cells detected by transwell assay and wound healing assay. LC cells transfected with miR-124 showed significantly suppressed migration (magnification x 10) **A-B**, and invasion (magnification x 40) **C-D** of LC cells. (**p<0.01 *vs.* control group, $^{\#}p$<0.05 *vs.* miR-124 mimic group).

ment of gene chip technology, increasingly more studies[28,29] have focused on the mechanism of the occurrence and development of LC at genetic and molecular levels. This is of great significance for clinical diagnosis and treatment of LC. Currently, the treatment of LC is mainly based on surgery combined with radiotherapy or chemotherapy. Early LC can be clinically cured by surgery combined with radiotherapy. However, middle-advanced LC is mainly treated with surgery combined with chemotherapy, whose therapeutic effect is far from satisfactory[30,31].

MiRNAs are a class of molecules with a wide range of regulatory functions in the body. They can regulate the products of 1/3 of the human genome[32]. The regulation of miRNA *in vivo* forms a complex network structure, in which a single miRNA can regulate multiple target genes. Meanwhile, a single protein gene can be regulated by multiple miRNAs simultaneously[33]. Based on previous researches[21-26], we selected miR-124 as the research object. In this study, we first examined the expression level of miRNA-124 in LC tissues and cells. The results demonstrated that miRNA-124 expression was significantly downregulated in LC tissues and cells.

Since miRNAs act by binding to the 3'-UTR of protein-expressing genes, we further exploited the downstream target gene of miR-124 and investigated the biological impact of the target gene on LC. Bioinformatics website (TargetScan and miRDB) predicted that PLOD2 was highly likely to be a target gene for miR-124 in LC. Hence, we constructed WT and MUT PLOD2 plasmid vectors. The targeted regulation relationship between miR-124 and PLOD2 was confirmed by Dual-Luciferase Reporter Gene Assay. The results showed that PLOD2 was the target gene of miR-124. Subsequent Western blot assay found that high or low expression of miR-124 could significantly influence the protein expression level of PLOD2 in LC. However, the changes in the expression of miR-124 had no significant effect on the mRNA expression of PLOD2.

PLOD2 gene is located between chromosomes 3q21 and 3q26, which mainly exists in the rough endoplasmic reticulum[34,35]. Dong et al[36] have found that PLOD2 is highly expressed in glioma tissues and is related to the prognosis of glioma patients. Researchers have compared the gene expression profile of tumor specimens of bladder cancer patients. The results have detected

that PLOD2 is highly expressed in patients with recurrent bladder cancer, which can be regarded as an effective predictor for early bladder cancer recurrence[37]. In addition, Rajkumar et al[38] have indicated that multiple genes, including PLOD2 protein, is highly expressed in cervical cancer and CIN3/carcinoma *in situ* compared with CIN1/CIN2 and normal cervical tissues. These findings suggest that PLOD2 is closely associated with the progression of cervical cancer. Moreover, PLOD2 protein can also enhance the expression of matrix metalloproteinase, thereby promoting the degradation of the tumor extracellular matrix. This may help to eliminate the physical barriers to invasion and migration of tumor cells[39]. However, no report has revealed the functional role of PLOD2 in the occurrence and development of LC.

To observe the potential role of PLOD2 in the development of LC, the rescue assays were designed in our study. The results found that the overexpression of PLOD2 could partly restore the inhibitory effects in Hep-2 cells induced by miR-124, confirming that PLOD2 was a functional target of miR-124.

Conclusions

We first demonstrated that miR-124 was lowly expressed in LC tissues and was involved in regulating the malignant behaviors of LC cells. Furthermore, the miR-124/PLOD2 axis might become a potential target for the treatment of LC.

Conflict of Interests

The authors declared that they have no conflict of interests.

References

1) Lombardi D, Accorona R, Lambert A, Mercante G, Coropciuc R, Paderno A, Lancini D, Spriano G, Nicolai P, Vander Poorten V. Long-term outcomes and prognosis in submandibular gland malignant tumors: a multicenter study. Laryngoscope 2018; 128: 2745-2750.
2) Zhou YH, Huang YY, Ma M. MicroRNA-138 inhibits proliferation and induces apoptosis of laryngeal carcinoma via targeting MAPK6. Eur Rev Med Pharmacol Sci 2018; 22: 5569-5575.
3) Yang M, Yang XM, Yin DH, Tang QL, Wang L, Huang C, Li P, Li SS. Beclin1 enhances cisplatin-induced apoptosis via Bcl-2-modulated autophagy in laryngeal carcinoma cells Hep-2. Neoplasma 2018; 65: 42-48.
4) Algazao JN, Akrami K, Martinez F, McCutchan A, Bharti AR. Saccharomyces cerevisiae laryngitis and oral lesions in a patient with laryngeal carcinoma. Case Rep Infect Dis 2017; 2017: 2941527.
5) Dankbaar JW, Oosterbroek J, Jager EA, de Jong HW, Raaijmakers CP, Willems SM, Terhaard CH, Philippens ME, Pameijer FA. Detection of cartilage invasion in laryngeal carcinoma with dynamic contrast-enhanced CT. Laryngoscope Investig Otolaryngol 2017; 2: 373-379.
6) Geng J, Lei YR, Pei SG. Correlation between survivin expression and laryngeal carcinoma: a meta-analysis. J Huazhong Univ Sci Technolog Med Sci 2017; 37: 965-973.
7) Yener HM, Yilmaz M, Karaaltin AB, Inan HC, Turgut F, Gozen ED, Comunoglu N, Karaman E. The incidence of thyroid cartilage invasion in early-stage laryngeal carcinoma: our experience on sixty-two patients. Clin Otolaryngol 2018; 43: 388-392.
8) Bartel DP. MicroRNAs: genomics, biogenesis, mechanism, and function. Cell 2004; 116: 281-297.
9) Kasschau KD, Xie Z, Allen E, Llave C, Chapman EJ, Krizan KA, Carrington JC. P1/HC-Pro, a viral suppressor of RNA silencing, interferes with Arabidopsis development and miRNA unction. Dev Cell 2003; 4: 205-217.
10) Lai EC, Wiel C, Rubin GM. Complementary miRNA pairs suggest a regulatory role for miRNA:miRNA duplexes. RNA 2004; 10: 171-175.
11) Murchison EP, Hannon GJ. MiRNAs on the move: miRNA biogenesis and the RNAi machinery. Curr Opin Cell Biol 2004; 16: 223-229.
12) Yoo JK, Lee JM, Kang SH, Jeon SH, Kim CM, Oh SH, Kim CH, Kim NK, Kim JK. The novel microRNA hsa-miR-CHA1 regulates cell proliferation and apoptosis in human lung cancer by targeting XIAP. Lung Cancer 2019; 132: 99-106.
13) Ding D, Qi Z. Clinical significance of miRNA-195 expression in patients with laryngeal carcinoma. J BUON 2019; 24: 315-322.
14) Watterston C, Zeng L, Onabadejo A, Childs SJ. MicroRNA26 attenuates vascular smooth muscle maturation via endothelial BMP signalling. PLoS Genet 2019; 15: e1008163.
15) Jin A, Bao R, Roth M, Liu L, Yang X, Tang X, Yang X, Sun Q, Lu S. MicroRNA-23a contributes to asthma by targeting BCL2 in airway epithelial cells and CXCL12 in fibroblasts. J Cell Physiol 2019; 234: 21153-21165.
16) Shen DW, Li YL, Hou YJ, Xu ZD, Li YZ, Chang JY. MicroRNA-543 promotes cell invasion and impedes apoptosis in pituitary adenoma via activating the Wnt/beta-catenin pathway by negative regulation of Smad7. Biosci Biotechnol Biochem 2019; 83: 1035-1044.
17) Hu J, Li L, Chen H, Zhang G, Liu H, Kong R, Chen H, Wang Y, Li Y, Tian F, Lv X, Li G, Sun B. MiR-361-3p regulates ERK1/2-induced EMT via DUSP2 mRNA degradation in pancreatic ductal adenocarcinoma. Cell Death Dis 2018; 9: 807.
18) Huang X, Xie X, Liu P, Yang L, Chen B, Song C, Tang H, Xie X. Adam12 and lnc015192 act as ceRNAs in breast cancer by regulating miR-34a. Oncogene 2018; 37: 6316-6326.

19) Vannini I, Wise PM, Challagundla KB, Plousiou M, Raffini M, Bandini E, Fanini F, Paliaga G, Crawford M, Ferracin M, Ivan C, Fabris L, Davuluri RV, Guo Z, Cortez MA, Zhang X, Chen L, Zhang S, Fernandez-Cymering C, Han L, Carloni S, Salvi S, Ling H, Murtadha M, Neviani P, Gitlitz BJ, Laird-Offringa IA, Nana-Sinkam P, Negrini M, Liang H, Amadori D, Cimmino A, Calin GA, Fabbri M. Transcribed ultraconserved region 339 promotes carcinogenesis by modulating tumor suppressor microRNAs. Nat Commun 2017; 8: 1801.
20) Vosgha H, Ariana A, Smith RA, Lam AK. MiR-205 targets angiogenesis and EMT concurrently in anaplastic thyroid carcinoma. Endocr Relat Cancer 2018; 25: 323-337.
21) Hu XX, Feng J, Huang XW, Lu PZ, Wang ZX, Dai HQ, Deng JH, Ye XP, Peng T, Hooi SC, Zhou J, Lu GD. Histone deacetylases up-regulate C/EBPα expression through reduction of miR-124-3p and miR-25 in hepatocellular carcinoma. Biochem Biophys Res Commun 2019; 514: 1009-1016.
22) Xu Y, Lai Y, Weng H, Tan L, Li Y, Chen G, Luo X, Ye Y. MiR-124 sensitizes cisplatin-induced cytotoxicity against CD133(+) hepatocellular carcinoma cells by targeting SIRT1/ROS/JNK pathway. Aging (Albany NY) 2019; 11: 2551-2564.
23) Long HD, Ma YS, Yang HQ, Xue SB, Liu JB, Yu F, Lv ZW, Li JY, Xie RT, Chang ZY, Lu GX, Xie WT, Fu D, Pang LJ. Reduced hsa-miR-124-3p levels are associated with the poor survival of patients with hepatocellular carcinoma. Mol Biol Rep 2018; 45: 2615-2623.
24) Wang Z, Dai J, Yan J, Zhang Y, Yin Z. Targeting EZH2 as a novel therapeutic strategy for sorafenib-resistant thyroid carcinoma. J Cell Mol Med 2019; 23: 4770-4778.
25) Zhou H, Tang K, Liu H, Zeng J, Li H, Yan L, Hu J, Guan W, Chen K, Xu H, Ye Z. Regulatory network of two tumor-suppressive noncoding RNAs interferes with the growth and metastasis of renal cell carcinoma. Mol Ther Nucleic Acids 2019; 16: 554-565.
26) Tang LX, Chen GH, Li H, He P, Zhang Y, Xu XW. Long non-coding RNA OGFRP1 regulates LYPD3 expression by sponging miR-124-3p and promotes non-small cell lung cancer progression. Biochem Biophys Res Commun 2018; 505: 578-585.
27) Fujiwara H, Sato T, Okada N, Fujita T, Kojima T, Daiko H. Thoracoscopic esophagectomy with three-field lymphadenectomy for thoracic esophageal cancer in a patient with a double aortic arch: a report of a case. Surg Case Rep 2019; 5: 80.
28) Cui W, Meng W, Zhao L, Cao H, Chi W, Wang B. TGF-beta-induced long non-coding RNA MIR155HG promotes the progression and EMT of laryngeal squamous cell carcinoma by regulating the miR-155-5p/SOX10 axis. Int J Oncol 2019; 54: 2005-2018.
29) Yang J, Zhou L, Zhang Y, Zheng J, Zhou J, Wei Z, Zou J. DIAPH1 is upregulated and unhibits cell apoptosis through ATR/p53/caspase-3 signaling pathway in laryngeal squamous cell carcinoma. Dis Markers 2019; 2019: 6716472.
30) Djukic V, Milovanovic J, Jotic AD, Vukasinovic M, Folic MM, Ivanov SY, Satueva DB. Laser transoral microsurgery in treatment of early laryngeal carcinoma. Eur Arch Otorhinolaryngol 2019; 276: 1747-1755.
31) Lee NCJ, Kelly JR, An Y, Park HS, Judson BL, Burtness BA, Husain ZA. Radiation therapy treatment facility and overall survival in the adjuvant setting for locally advanced head and neck squamous cell carcinoma. Cancer 2019; 125: 2018-2026.
32) Cheng AM, Byrom MW, Shelton J, Ford LP. Antisense inhibition of human miRNAs and indications for an involvement of miRNA in cell growth and apoptosis. Nucleic Acids Res 2005; 33: 1290-1297.
33) Jay C, Nemunaitis J, Chen P, Fulgham P, Tong AW. MiRNA profiling for diagnosis and prognosis of human cancer. DNA Cell Biol 2007; 26: 293-300.
34) Uzawa K, Grzesik WJ, Nishiura T, Kuznetsov SA, Robey PG, Brenner DA, Yamauchi M. Differential expression of human lysyl hydroxylase genes, lysine hydroxylation, and cross-linking of type I collagen during osteoblastic differentiation in vitro. J Bone Miner Res 1999; 14: 1272-1280.
35) Ruotsalainen H, Vanhatupa S, Tampio M, Sipila L, Valtavaara M, Myllyla R. Complete genomic structure of mouse lysyl hydroxylase 2 and lysyl hydroxylase 3/collagen glucosyltransferase. Matrix Biol 2001; 20: 137-146.
36) Dong H, Cao W, Xue J. Long noncoding FOXD2-AS1 is activated by CREB1 and promotes cell proliferation and metastasis in glioma by sponging miR-185 through targeting AKT1. Biochem Biophys Res Commun 2019; 508: 1074-1081.
37) Mares J, Szakacsova M, Soukup V, Duskova J, Horinek A, Babjuk M. Prediction of recurrence in low and intermediate risk non-muscle invasive bladder cancer by real-time quantitative PCR analysis: cDNA microarray results. Neoplasma 2013; 60: 295-301.
38) Rajkumar T, Sabitha K, Vijayalakshmi N, Shirley S, Bose MV, Gopal G, Selvaluxmy G. Identification and validation of genes involved in cervical tumourigenesis. BMC Cancer 2011; 11: 80.
39) John AMSP, Kundu S, Pushpakumar S, Fordham M, Weber G, Mukhopadhyay M, Sen U. GYY4137, a hydrogen sulfide donor modulates miR194-dependent collagen realignment in diabetic kidney. Sci Rep 2017; 7: 10924.